Proceedings of IASS-IWSS 2026 — September 14-18, 2026, Turin, Italy
"R-Evolution of Shapes: Sustainability, Re-Use, and new Design Paradigms"
Annual Symposium of the International Association for Shell and Spatial Structures
3rd Italian Workshop on Shell and Spatial Structures
A. Manuello Bertetto, S. Gabriele, F. Marmo, A. Micheletti (eds.)

Economical and Environmental Optimization of Timber-Cable Photovoltaic Structures

Benjamin DARDENNE*, Pierre LATTEUR[a]

*[a]UCLouvain, IMMC - Institute of Mechanics, Materials and Civil Engineering
Place du levant 1/L5.05.01, Louvain-la-Neuve 1348, Belgium
*benjamin.dardenne@uclouvain.be

Abstract

The widespread deployment of photovoltaic power plants (PV) is essential to achieving carbon neutrality targets in Europe by 2050. New types of large-scale PV structures are emerging, such as canopies over parking lots, roads, channels, agricultural fields… requiring all structures capable of freeing up large spaces while minimizing economic and environmental impacts. Although steel is currently the predominant material, this study explores the potential of timber logs – an abundant, environmentally friendly, and economical material – as a sustainable alternative for load-bearing structures. The study presents a parametric optimization method based on the concept of morphological indicators (MI). MI allow simplifying complex design problems by grouping strength, geometry, and load variables into dimensionless ratios, which facilitates the identification of optimal configurations regardless of project scale. The study compares several structural configurations, with a particular focus on the use of cable trusses for long-span elements. The article shows that the use of logs for columns and support beams, combined with cable trusses, reduces construction costs and global warming potential (GWP) compared to conventional steel structures, which have a very unfavorable economic and ecological balance. In conclusion, the combination of timber logs and cables appears to be a viable solution for reconciling the ecological and economic objectives of photovoltaic developers, while offering a natural aesthetic that promotes landscape integration and social acceptability of these infrastructures.

Keywords: Morphological indicators, Optimization, Photovoltaic, Cable truss, Wood, Tree logs, Timber, Steel

1. Introduction

Photovoltaics (PV) needs to reinvent itself to ensure sufficient energy production complying with the goals of the European Government. Aside from PV panels on top of our roofs, large power plants have exciting potential to provide electricity but occupy a lot of ground space. Combining them with another activity such as parking lot, roads or agricultural fields is a good compromise, enabling energy production while still allowing the use of a significant space [1], [2]. This can be achieved by putting the panels several meters above the ground, similar to canopies. Such canopies feature widely spaced column grid and elevated panel height, as illustrated by the steel-cable canopy built of Figure 1.

Steel is currently the predominant material for the load-bearing structures of these canopies, valued for its consistency, ease of design and recyclability. However, steel carries a significant carbon footprint, is relatively expensive, and may appear unappealing in the landscape, especially in rural landscapes [3], [4], [5]. As an alternative, timber logs – raw, minimally processed wood – offer lower cost, a substantially reduced environmental impact, and a natural aesthetic [6], [7].

This study presents a parametric optimization method based on morphological indicators (MI) [8], [9], [10], [11] to compare steel and timber structures for PV canopies [4]. The objective is to minimize both installation cost and Global Warming Potential (GWP) [12] of the supporting structure.

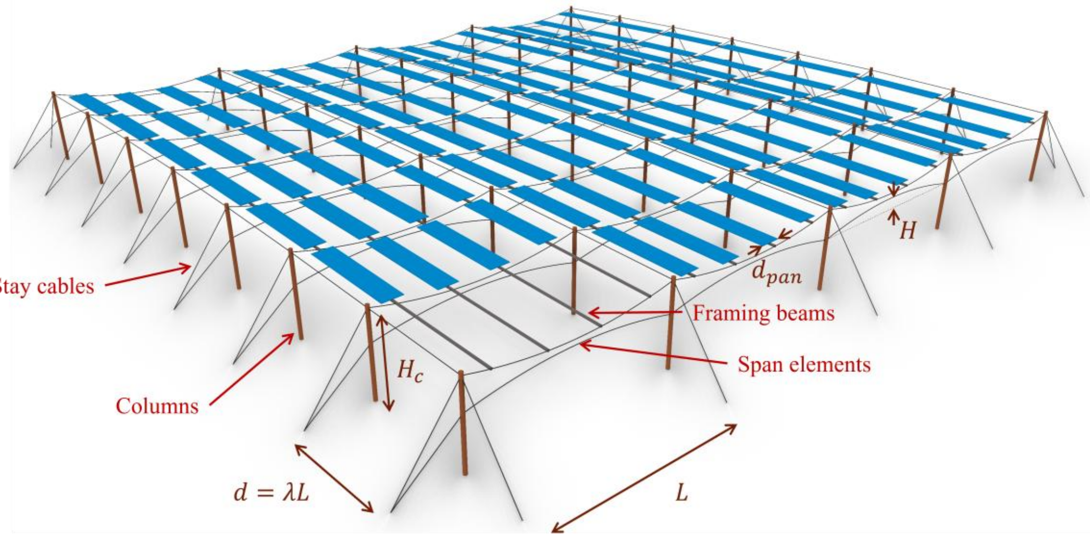

Figure 1: Schematic PV canopy considered in this study.

2. Structural model and assumptions

A PV canopy is composed of a repetition of identical modules of dimensions $d \times L \times H_c$, as shown on Figure 1. Each module consists of four structural element categories: (i) columns of height H_c, hinged at both ends and subjected only to compression; (ii) span elements along the long span L, which can be a cable truss (as on Figure 1) or a rigid beam; (iii) framing beams along the short span d $(= \lambda L)$, supporting the solar panels; and (iv) stay cables and foundations, excluded from the optimization scope.

Only static loads are considered at Ultimate Limit State (ULS) following Eurocode 1 [13], [14], [15]. The design surface load q_{pan} (N/m^2) includes panel's self-weight, snow, and wind. The loads considered are shown at Figure 2, with the Ground Coverage Ratio ζ (panel area/ground area). Four cross-section types are studied: full circular (timber log), hollow circular steel tube, hollow square steel tube, and steel I-section (see Figure 3). Cable trusses use high-strength steel strands (see Figure 4).

The mechanical properties used are: timber D30 (bending $f = 30\ MPa$, compression $f = 24\ MPa$, $E = 9200\ MPa$, $\gamma = 1.86$); structural steel S355 ($f = 355\ MPa$, $\gamma = 1$); steel cable ($f = 1{,}500\ MPa$, $\gamma = 1$). The Ground Coverage Ratio ζ is kept constant at 30 %.

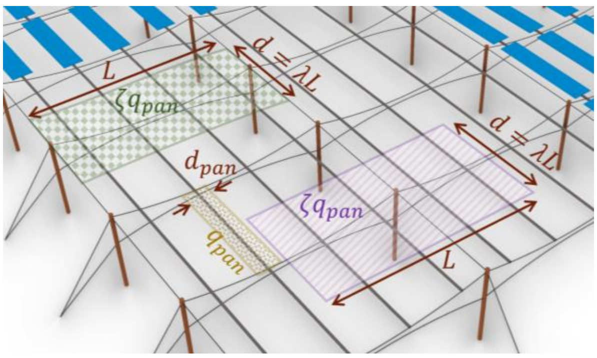

Figure 2: Loads on the PV canopy's structural elements.

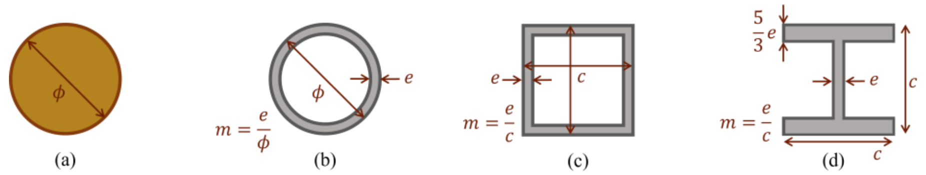

Figure 3: (a) Full circular section, (b) Empty circular section, (c) Empty square section and (d) I-section with proportions similar to a HEB cross-section.

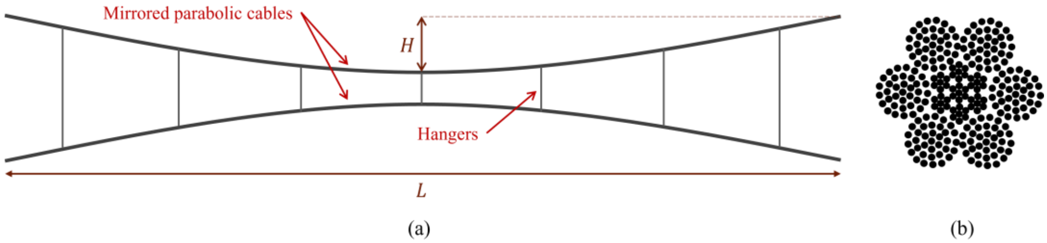

Figure 4: a) Cable truss b) Possible steel cable's cross-section [16].

3. Morphological indicators

Morphological indicators (MI) are dimensionless numbers that group design variables – material strength, geometry, and loading – enabling identification of optimal structural configurations independently of project scale. The volume indicator for a module as shown at Figure 1 is defined as:

$$\Xi = \frac{V}{L^3} \quad Eq. 1$$

For a complete PV module: $\Xi_{module} = \Xi_{fr} + \Xi_{sp} + \Xi_c$, where subscripts "fr", "sp", "c" denote respectively "framing beams", "span elements", and "columns". Each term is multiplied by a material coefficient C_{price} ($€/m^3$) or C_{GWP} ($kgCO2eq/m^3$). Reference values would be: timber logs: 500 $€/m^3$ and 75 $kgCO2eq/m^3$; structural steel: 31 400 $€/m^3$ and 20 000 $kgCO2eq/m^3$; steel cables: 26 000 $€/m^3$ and 20 000 $kgCO2eq/m^3$ [16], [17], [18], [19].

Three dimensionless parameters are defined to simplify the expressions of the indicators: $R = q_{pan}\gamma/f$ (material strength indicator); $\alpha = A/W_{el}^{2/3}$ (cross-section shape indicator); $\psi = f_c H_c A_c / \sqrt{E_c I_c \zeta q_{pan} dL}$ (column buckling indicator). The derived volume indicators are for each structural category are:

- Framing beams: $\Xi_{fr} = \frac{V_{fr}}{L^3} = \frac{1}{4}\zeta\alpha\left(\frac{L}{d_{pan}}\right)^{\frac{1}{3}} R^{\frac{2}{3}}\lambda^{\frac{7}{3}} \quad Eq. 2$
- Span cable truss: $\Xi_{sp} = \frac{V_{sp}}{L^3} = \frac{1}{8}\zeta R\lambda\frac{L}{H}\kappa\left(\kappa + \frac{L}{4H}\ln\left[\frac{4H}{L} + \kappa\right]\right) \quad Eq. 3$
- Span beam: $\Xi_{sp} = \frac{V_{sp}}{L^3} = \frac{1}{4}\zeta^{\frac{2}{3}}\alpha R^{\frac{2}{3}}\lambda^{\frac{2}{3}} \quad Eq. 4$
- Column: $\Xi_c = \frac{V_c}{L^3} = \frac{1}{2}\zeta\lambda\frac{H_c}{L}R\left(1 + \sqrt{1 + \frac{4}{\pi^2}\frac{1}{\zeta}\psi^2}\right) \quad Eq. 5$

where $\lambda = d/L$ and $\kappa = \sqrt{1 + (4H/L)^2}$. For the detailed development of those expressions, see *Dardenne et al* [4].

4. Comparison of structural elements

Price and GWP indicators are plotted as functions of λ, for $\zeta = 30\,\%$, $L/dpan = 15$, $L/H_c = 3.75$, $L/H = 20$, and $m = 0.05$. Those values are considered to be an average reality.

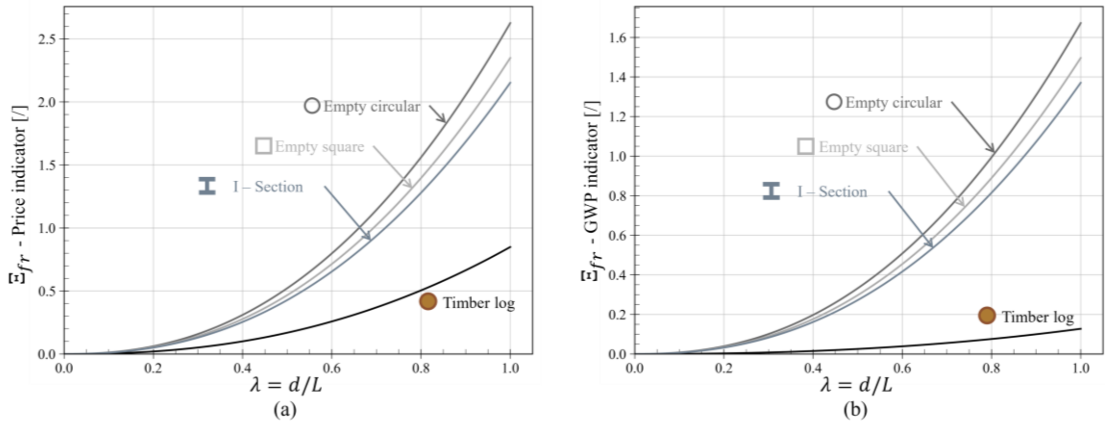

Figure 5 : Comparison of Ξ_{fr} of the framing elements regarding the (a) price and the (b) GWP.

Figure 5 shows the evolution of the framing beams indicator Ξ_{fr} in function of the geometrical parameter λ. Timber logs consistently yield lower price and GWP indicators than all steel cross-sections, regardless of λ. The combined effect of lower material price and carbon footprint makes timber the clear choice for framing elements.

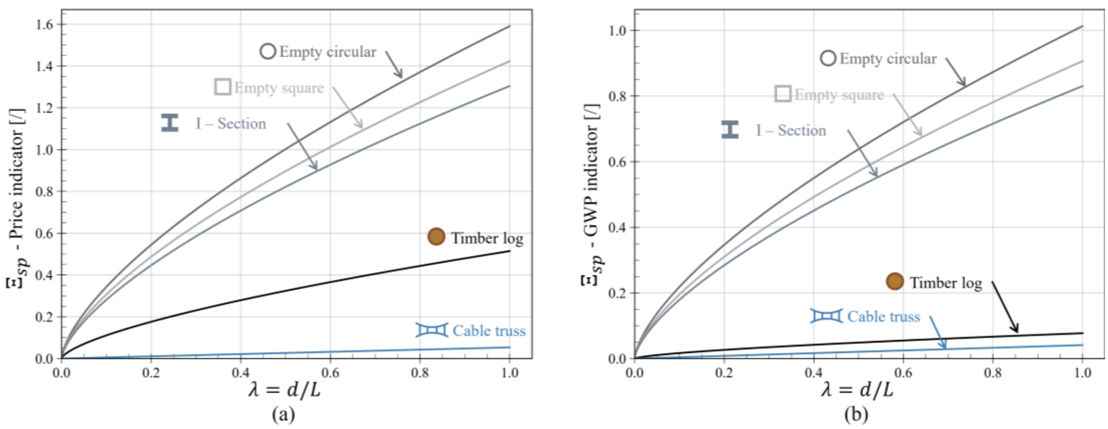

Figure 6 : Comparison of Ξ_{sp} of the span elements regarding the (a) price and the (b) GWP.

Figure 6 shows that timber logs outperform steel rigid beams in both criteria when used as span elements. However, cable trusses outperform all rigid sections – whether timber or steel – because the extremely high tensile strength of steel cables enables minimal material usage over long spans. Cable trusses are therefore the optimal span element.

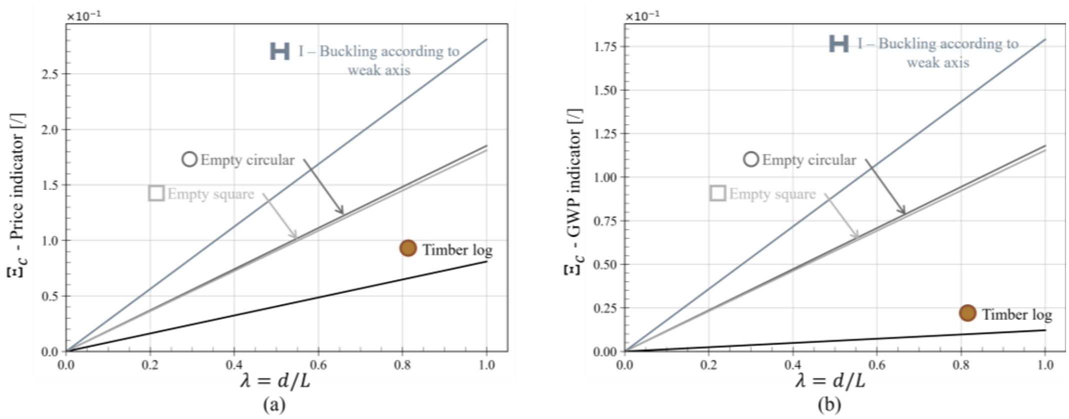

Figure 7 : Comparison of Ξ_c of column regarding the (a) price and (b) GWP.

Figure 7 highlights that the same trend for span and framing elements holds for columns: timber logs yield lower price and GWP indicators than steel tubes or I-sections. Despite requiring larger cross-sections [4], the much lower cost and GWP per unit volume of wood more than compensates.

5. Comparison of four PV configurations

Four complete module configurations are compared: (1) Timber logs for framing and columns with cable truss for spans; (2) All-timber; (3) Steel I-sections for framing and columns with cable truss for spans; (4) All-steel (current industry standard). Table 1 details those configurations.

Table 1: PV plant configurations considered in the following of this study and the associated weighting coefficients.

	Framing elements	Span elements	Column
Configuration 1	Timber log (C_{price} = 500, C_{GWP} = 75)	Cable truss (C_{price} = 26000, C_{GWP} = 20000)	Timber log (C_{price} = 500, C_{GWP} = 75)
Configuration 2	Timber log (C_{price} = 500, C_{GWP} = 75)	Timber log (C_{price} = 500, C_{GWP} = 75)	Timber log (C_{price} = 500, C_{GWP} = 75)
Configuration 3	I – Section (C_{price} = 31400, C_{GWP} = 20000)	Cable truss (C_{price} = 26000, C_{GWP} = 20000)	Empty square (C_{price} = 31400, C_{GWP} = 20000)
Configuration 4	I – Section (C_{price} = 31400, C_{GWP} = 20000)	I – Section (C_{price} = 31400, C_{GWP} = 20000)	Empty square (C_{price} = 31400, C_{GWP} = 20000)

Results show that configurations 1 and 2 (timber-based) are 2 to 3 times less expensive than configurations 3 and 4 (steel-based). In terms of GWP, timber configurations outperform steel ones by a factor of 4 to 8. Configuration 1 – timber logs with cable trusses – is consistently the best performer. Configuration 4, the most widespread today, shows the worst economic and ecological performance.

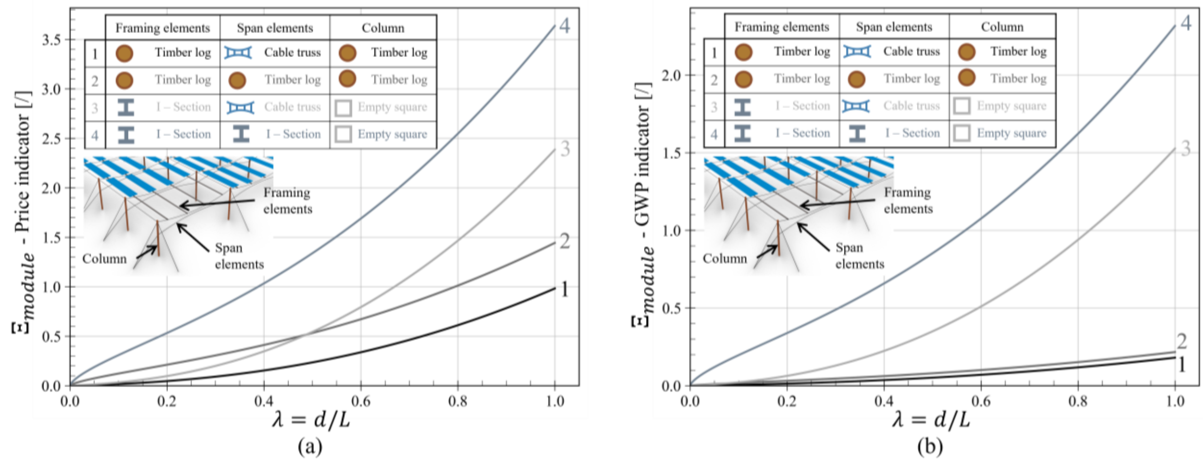

Figure 8: Indicator Ξ_{module} of (a) price and (b) GWP for an entire module with different combinations of structural element's cross-sections.

Material prices and Global Warming Potential (GWP) can vary across countries and over time, depending on the prevailing economic conditions. In some cases, materials may need to be imported over long distances, particularly in remote locations. Additionally, material costs can rise significantly, as observed for timber in 2021, when prices nearly doubled in many countries of Europe [20]. Figure 9 shows the volume indicator Ξ of configuration 1 and 3 if the price or GWP would come to double or halve in a defavorable way for timber elements and favorable for steel ones as detailed in Table 2.

Table 2: Reference and modified weighting coefficients C_{price} and C_{GWP} used for the different configurations of Table 1.

Configurations as in Table 1 :	1	1'	3	3'
$C_{price,fr}$	500	→ ×2 1000	31400	→ ÷2 15700
$C_{price,span}$	26000	→ ÷2 13000	26000	→ ÷2 13000
$C_{price,c}$	500	→ ×2 1000	31400	→ ÷2 15700
$C_{GWP,fr}$	75	→ ×2 150	20000	→ ÷2 10000
$C_{GWP,span}$	20000	→ ÷2 10000	20000	→ ÷2 10000
$C_{GWP,c}$	75	→ ×2 150	20000	→ ÷2 10000

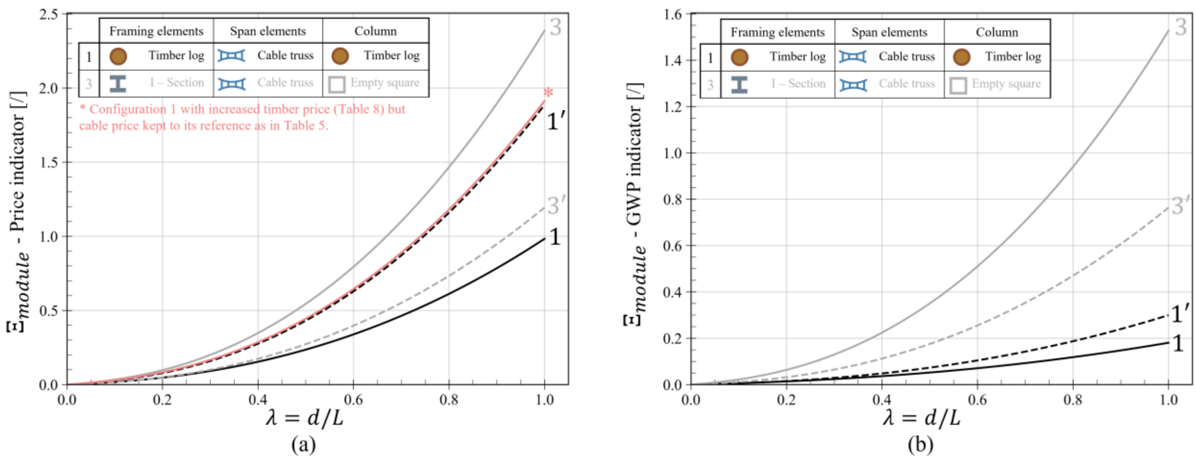

Figure 9: Comparison of the indicator Ξ_{module} of (a) price and (b) GWP for the configuration 1 and 3 of the Table 1 when the price or GWP of the materials vary.

Figure 9 shows that even if timber prices double and steel prices simultaneously halve, going from configuration 1 and 3 to respectively 1′ and 3′, timber-based structures still outperform steel on GWP, and remain competitive on cost. The dominance of timber holds across the realistic range of geometric parameters: L/d_{pan} from 8 to 40, L/H_c from 1 to 5, L/H from 2 to 40.

6. Discussion

Prestressing of the cable truss is required to ensure stiffness and limit vibrations [21]. Figure 6 shows a clear massive difference in price and GWP of cable trusses compared to the other cross-sections. The limited increase in volume induced by the increase of prestressing would have minimal effect on the overall module indicator, confirming that prestressing can be neglected at the preliminary design stage.

Serviceability limit state (deflection) was excluded for several reasons. Stiffness can be increased thanks to prestressing but assessing the displacements would need advanced non-linear software, outside of the scope of this study. Moreover, displacement criteria PV structures are not well established.

Foundations and peripheral stay cables were also excluded, as all four configurations require similar provisions and their inclusion would not change the relative conclusions drawn.

Service time of a PV plant is typically 20 years [15]. Timber durability over a 20-year service life is achievable when naturally durable species (oak, black locust, chestnut) are used or when less durable species receive preservative treatment [13]. Even accounting for a mid-life replacement of timber elements – effectively doubling cost and GWP – timber structures remain more economical and environmentally friendly than steel counterparts, as demonstrated at Figure 9. Considering steel connectors for timber joints can increase costs, but doubling the timber price to account for connections, timber remains less expensive than steel.

7. Conclusion

This study shows that photovoltaic canopies using timber logs and cable trusses are 2 to 3 times more economical and 4 to 10 times more environmentally sustainable (in GWP) than conventional steel structures.

The morphological indicator method transforms a complex multi-parameter optimization into a family of dimensionless curves, enabling rapid comparison of configurations independently of project scale. The optimal configuration combines timber log columns and framing beams with steel cable trusses for long spans, as represented at Figure 1.

The potential shift in the materials prices and GWP are predictable and do not change the conclusion on the superiority of timber-based structures over their steel counterparts.

Further work should address the dynamic wind response of cable-supported PV canopies, where prestressing plays a more significant role.

Acknowledgements

This work was supported by the Wallonia Research SPW [Agreement 2210193] and the LEMSC – Laboratoire Essais Mécaniques, Structures et génie Civil – UCLouvain. The authors thank Andrea Di Maria (Gembloux Agro-Bio Tech, ULiège) for his help with environmental impact calculations and access to the Ecoinvent database. Thanks also to Dorothée Stiermon and Catherine Massart from the LAB *Architecture et Climat* – UCLouvain, who took the time to discuss the challenges involved in the environmental analysis.

References

[1] C. Dupraz, H. Marrou, G. Talbot, L. Dufour, A. Nogier, et Y. Ferard, « Combining solar photovoltaic panels and food crops for optimising land use: Towards new agrivoltaic schemes », *Renewable Energy*, vol. 36, nº 10, p. 2725-2732, oct. 2011, doi: 10.1016/j.renene.2011.03.005.

[2] A. Goetzberger et A. Zastrow, « On the Coexistence of Solar-Energy Conversion and Plant Cultivation », *International Journal of Solar Energy*, janv. 1982, doi: 10.1080/01425918208909875.

[3] B. Dardenne et P. Latteur, « Structural optimisation of free-swinging agrivoltaic fences », *Renewable and Sustainable Energy Reviews*, vol. 210, p. 115160, mars 2025, doi: 10.1016/j.rser.2024.115160.

[4] B. Dardenne, *Timber and steel agri-photovoltaic canopies: environmental and cost optimization*. 2026. doi: 10.13140/RG.2.2.36427.55842.

[5] A. Laurent, Y. van der Meer, et C. Villeneuve, « Comparative Life Cycle Carbon Footprint of a Non-Residential Steel and Wooden Building Structures », déc. 2018, doi: 10.29011/2638-0013.100028.

[6] J. Geno, J. Goosse, S. Van Nimwegen, et P. Latteur, « Parametric design and robotic fabrication of whole timber reciprocal structures », *Automation in Construction*, vol. 138, p. 104198, juin 2022, doi: 10.1016/j.autcon.2022.104198.

[7] M. Steinmetz, P. Latteur, et L. Sgambi, « Optimal log floor patterns », *Engineering Structures*, vol. 297, p. 116970, déc. 2023, doi: 10.1016/j.engstruct.2023.116970.

[8] P. Latteur, *Calculer une structure, de la théorie à l'exemple*. 2016. Consulté le: 22 mai 2024. [En ligne]. Disponible sur: https://dial.uclouvain.be/pr/boreal/fr/object/boreal%3A185696

[9] P. Latteur, « Optimisation et prédimensionnement des treillis, arcs, poutres et câbles sur base d'indicateurs morphologiques; application aux structures soumises en partie ou en totalité au flambement », *Optimization and Design of trusses, arches, beams and cables with morphological indicators*, mai 2000, Consulté le: 11 juillet 2024. [En ligne]. Disponible sur: https://orbi.uliege.be/handle/2268/30107

[10] P. Samyn, *Étude de la morphologie des structures: à l'aide des indicateurs de volume et de déplacement*. Classe des sciences, Académie royale de Belgique, 2004.

[11] B. Dardenne et X. de Liedekerke de Pailhe, « Conception et optimisation de structures agrivoltaïques via modélisation paramétrique : câbles et grumes, allier légèreté et simplicité », 2023.

[12] « Glossary:Global-warming potential (GWP) ». Consulté le: 24 janvier 2025. [En ligne]. Disponible sur: https://ec.europa.eu/eurostat/statistics-explained/index.php?title=Glossary:Global-warming_potential_(GWP)

[13] « Eurocode 5 : Calcul des structures en Bois | Eurocodes: Building the future ». Consulté le: 10 juillet 2025. [En ligne]. Disponible sur: https://eurocodes.jrc.ec.europa.eu/events/eurocode-5-calcul-des-structures-en-bois?id=562

[14] « NBN EN 1991-1-4:2005 - NBN ». Consulté le: 29 août 2025. [En ligne]. Disponible sur: https://app.nbn.be/data/r/platform/frontend/detail?p40_id=177420&p40_language_code=en&p40_detail_id=1316105&session=3438124297693

[15] « NBN EN 1991-1-1:2025 - EN ». Consulté le: 1 avril 2026. [En ligne]. Disponible sur: https://app.nbn.be/data/r/platform/frontend/detail?p40_id=2690924&p40_language_code=en&p40_detail_id=1470852&session=7618098103317

[16] « Nos câbles », Câbleries Namuroises. Consulté le: 9 janvier 2025. [En ligne]. Disponible sur: https://www.cabnam.be/fr/catalogue-detail/GA6x36%20A

[17] « Poutrelles grenaillées prépeintes | Aciers Grosjean ». Consulté le: 9 janvier 2025. [En ligne]. Disponible sur: https://pro.aciersgrosjean.be/public/21

[18] « Site, Forêts à vendre, étang, haras, indicateur de marché forestier, cours du bois, carte de France, sépartements, région ». Consulté le: 23 mai 2024. [En ligne]. Disponible sur: https://www.europeansa-online.com/bois_sur_pied.php

[19] « Database », ecoinvent. Consulté le: 23 janvier 2025. [En ligne]. Disponible sur: https://ecoinvent.org/database/

[20] « Lumber - Price - Chart - Historical Data - News ». Consulté le: 8 juillet 2025. [En ligne]. Disponible sur: https://tradingeconomics.com/commodity/lumber

[21] M. Acic, L. Vlajic, et D. Kostic, « Determination of prestressing levels for cable trusses as a function of their stability », *Gradevinar*, vol. 65, p. 1097-1110, déc. 2013, doi: 10.14256/JCE.863.2013.